Two new hybrid compounds assembled from Keggin-type polyoxometalates and transition metal coordination complexes

Yan Wang [a], Bo Zou [b], Li-Na Xiao [a], Ning Jin [c], Yu Peng [a], Feng-Qing Wu [b], Hong Ding [a], Tie-Gang Wang [a], Zhong-Min Gao [a], Da-Fang Zheng [a], Xiao-Bing Cui [a,*], Ji-Qing Xu [a,*]

[a] College of Chemistry and State Key Laboratory of Inorganic Synthesis and Preparative Chemistry, Jilin University, Changchun 130023, China
[b] College of Chemistry, Jilin University, Changchun 130023, China
[c] China–Japan Union Hospital of Jilin University, Changchun, China

ARTICLE INFO

ABSTRACT

Two new hybrid compounds based on Keggin-type polyoxometalates: $\{[PMo_{12}O_{40}][Ni(Phen)_2(H_2O)]_2\} \cdot K \cdot 2OH^-$ (1) and $[Cd_2(Phen)_4Cl_2][HPW_{12}O_{40}] \cdot H_2O$ (2) (Phen=1,10-phenanthroline), have been prepared and characterized by IR, UV–vis, XPS, XRD and single crystal X-ray diffraction analyses. Compound 1 exhibits a 1-D chain structure constructed from Pseudo-Keggin polyoxometalate bi-supported transition metal coordination complexes linked by K^+ ions. Compound 2 contains Pseudo-Keggin polyoxoanions $[HPW_{12}O_{40}]^{2-}$ and novel metal–chloride–ligand coordination complexes $[Cd_2(Phen)_4Cl_2]^{2+}$.

© 2011 Elsevier Inc. All rights reserved.

1. Introduction

It has been widely recognized that the polyoxometalates (POMs) exhibit a variety of structures and properties that make them useful in catalysis, material science and medicine [1–6]. Recently a new advance in the POM chemistry is that a large number of hybrid compounds with unprecedented structures constructed from the combination of POMs and transition metal coordination complexes (TMCs) have been obtained [7–12]. An intelligent choice of POMs and TMCs may yield materials with fascinating structures and desirable properties. The diversity of POM building blocks and TMCs has led to a wide array of functional organic–inorganic hybrid materials. The POMs interact with the TMCs through covalent or non-covalent supramolecular interactions, leading to numerous extended structures or supramolecular structures [7–12].

Up to now, most of existing POMs have already been applied to be combined with TMCs into hybrids, including Keggin, Dawson POMs, etc. Doubtless, of which the Keggin one is the most widely used to be combined with different TMCs into hybrids. Thus, it is a popular strategy to employ different TMCs to be combined with the Keggin POMs for hybrid materials. Based on this strategy, a number of hybrid compounds have been reported [13].

Our group has focused on hybrids based POMs and transition metal coordination complexes for years. As part of the continuing work in this system, in this paper, we reported two new hybrid compounds based on Keggin polyoxometalates: $\{[PMo_{12}O_{40}][Ni(Phen)_2(H_2O)]_2\} \cdot K \cdot 2OH^-$ (1) and $[Cd_2(Phen)_4Cl_2][HPW_{12}O_{40}] \cdot H_2O$ (2). Compound 1 is a 1-D chain structure which is constructed from Keggin POM supported transition metal coordination fragments linked by alkali metals. Compound 2 is constructed from Keggin POMs and transition metal–halide–organic coordination units.

2. Experimental section

2.1. Material and measurement

All reagents were purchased commercially and used without further purification. Elemental analyses (C, H and N) were performed on a Perkin-Elmer 2400 Series II CHNS/O elemental analyzer. The elemental analyses of Mo, W, Cl, Ni and Cd were determined by inductively coupled plasma (ICP) analyses on a Perkin-Elmer Optima 3300DV ICP spectrometer. The infrared spectra were recorded with a Perkin-Elmer SPECTRUM ONE FTIR

spectrometer with KBr pellets in the 4000–200 cm^{-1} region. XPS measurements were performed on single crystals with ESCALAB MARK II apparatus, using the Mg$K\alpha$ (1253.6 eV) achromatic X-ray radiation source. The powder XRD patterns were obtained with a Scintag X1 powder diffractometer system using Cu$K\alpha$ radiation with a variable divergent slit and a solid-state detector. The UV–vis spectra were recorded on a Shimadzu UV3100 spectrophotometer.

2.2. Syntheses

2.2.1. Synthesis of {[PMo$_{12}$O$_{40}$][Ni(Phen)$_2$(H$_2$O)]$_2$}·K·2OH$^-$ (1)

Compound **1** was synthesized hydrothermally by reacting of Na$_2$WO$_4$·2H$_2$O (0.5 g, 1.5 mmol), (NH$_4$)$_6$Mo$_7$O$_{24}$·2H$_2$O(0.5 g, 0.4 mmol), KH$_2$PO$_4$(0.2 g, 1.5 mmol), NiCl$_2$·2H$_2$O (0.3 g, 1.3 mmol), *Phen* (0.15 g, 0.8 mmol) and distilled water (15 ml) in a 18 ml Teflon-lined autoclave. The pH of the mixture was necessarily adjusted to 4 with HCl solution. The mixture was heated under autogenous pressure at 160 °C for 5 days and then left to cool to room temperature. Green crystals could be isolated in about 55% yield (based on Mo). The pH value of the final solution is about 6. We also tried to synthesize compound **1** without the addition of the Na$_2$WO$_4$·2H$_2$O, which is still unsuccessful. Na$_2$WO$_4$·2H$_2$O did not appear in the final product, which is common in the hydrothermal syntheses. We do believe that compound **1** could be yielded without the addition of Na$_2$WO$_4$·2H$_2$O, but the synthesis conditions will change very much (we have not found the conditions yet). However, under current conditions, Na$_2$WO$_4$·2H$_2$O is important for its influence of the ionic strength of the reaction solution. Anal. Calcd. for C$_{48}$H$_{38}$KMo$_{12}$N$_8$Ni$_2$O$_{44}$P: Mo, 41.57; P, 1.12; K, 1.41; Ni, 4.24; C, 20.82; H,1.38; N, 4.05%. Found: Mo, 41.47; P, 1.19; K, 1.27; Ni, 4.31; C, 20.73; H,1.42; N, 4.05%.

2.2.2. Synthesis of [Cd$_2$(Phen)$_4$Cl$_2$][HPW$_{12}$O$_{40}$]·H$_2$O (2)

Compound **2** was synthesized hydrothermally by reacting of Na$_2$WO$_4$·2H$_2$O (0.5 g, 1.5 mmol), KH$_2$PO$_4$(0.2 g, 1.5 mmol), CdCl$_2$·2.5H$_2$O (0.3 g, 1.3 mmol), *Phen* (0.15 g, 0.8 mmol) and distilled water (15ml) in a 18ml Teflon-lined autoclave. The pH of the mixture was necessarily adjusted to 4 with HCl solution. The mixture was heated under autogenous pressure at 160 °C for 5 days and then left to cool to room temperature. Yellow crystals could be isolated in 45% yield (based on W). Anal. Calcd for C$_{48}$H$_{35}$Cd$_2$Cl$_2$N$_8$O$_{41}$PW$_{12}$: W, 56.39; P, 0.79; Cd, 5.75; Cl, 1.81; C, 14.73; H, 0.90; N, 2.86%. Found: W, 56.26; P, 0.55; Cd, 5.62; Cl, 1.33; C, 14.41; H, 0.79; N, 2.87%.

2.3. X-ray crystallography

The reflection intensity data for compounds **1** and **2** were measured on a Rigaku R-AXIS RAPID IP diffractometer with graphite monochromated Mo$K\alpha$ ($\lambda=0.71073$ μ) radiation. Neither of the crystals showed evidence of crystal decay during the data collections. Both structures were solved by direct methods and refined using the full-matrix least squares on F^2 with SHELXTL-97 crystallographic software package. In the final refinements, all atoms were refined anisotropically except the P1, O1, O2, O3 and O4 atoms in compound **2**. The hydrogen atoms of the *Phen* ligands in compounds **1** and **2** were placed geometrically, while those of water molecules in compounds **1** and **2** and those of hydroxyl ions in compound **1** were not added. A summary of the crystallographic data and structure refinements for compounds **1** and **2** are given in Table 1. Selected bond lengths of compounds **1** and **2** are shown in Table 2. CCDC numbers: 791,833 for **1** and 791,834 for **2**. These data can be obtained free of charge from The Cambridge Crystallographic Data Center via www.ccdc.cam.ac. uk/data_request/cif.

Table 1
Crystal data and structural refinements for compounds **1** and **2**.

Empirical formula	C$_{48}$H$_{38}$KMo$_{12}$N$_8$Ni$_2$O$_{44}$P	C$_{48}$H$_{35}$Cd$_2$Cl$_2$N$_8$O$_{41}$PW$_{12}$
Formula weight	2769.59	3912.71
Crystal system	Triclinic	Monoclinic
Space group	$P-1$	$C2/c$
a (Å)	10.7462(6)	24.407(5)
b (Å)	13.2324(7)	12.198(2)
c (Å)	13.6528(8)	24.226(5)
α (deg)	69.4980(10)	90
β (deg)	71.7970(10)	98.27(3)
γ (deg)	79.0790(10)	90
Volume (Å^3)	1720.43(17)	7137(2)
Z	1	4
D_C (mg m^{-3})	2.673	3.641
μ (mm^{-1})	2.834	20.029
$F(000)$	1327	6960
θ for data collection	2.00–25.99	1.87–28.27
Limiting indices	$^-13 < h < =10$	$^-32 < h < =29$
	$^-16 < k < =16$	$^-13 < k < =16$
	$^-15 < l < =16$	$^-32 < l < =31$
Reflections collected	9545	24,949
Reflections unique	6667 [R(int)=0.0247]	8754 [R(int)=0.0831]
Completeness to θ	98.7%	98.8%
Data/parameters	6667/544	8754/509
GOF on F^2	1.034	1.053
R^a	$R_1=0.0674$	$R_1=0.0677$
[$I > 2\sigma(I)$]	$\omega R_2=0.1773$	$\omega R_2=0.1497$
R^b (all data)	$R_1=0.0849$	$R_1=0.1117$
	$\omega R_2=0.1899$	$\omega R_2=0.1699$

[a] $R_1=\sum||F_o|-|F_c||/\sum|F_o|$.
[b] $\omega R_2=\{\sum[w(F_o^2-F_c^2)^2]/\sum[w(F_o^2)^2]\}^{1/2}$.

3. Results and discussion

3.1. Crystal structures

3.1.1. Crystal structure of compound 1

Compound **1** contains [PMo$_{12}$O$_{40}$]$^{3-}$ ions, [Ni(*Phen*)$_2$(H$_2$O)]$^{2+}$ TMCs, potassium cations and hydroxyl ions. As shown in Fig. 1, [PMo$_{12}$O$_{40}$]$^{3-}$ may be viewed as a shell of {Mo$_{12}$O$_{36}$} encapsulating a disordered PO$_4$ moiety present at its center with P–O distances ranging from 1.523(18) to 1.550(18) Å. The Mo–O distances can be grouped into three sets: Mo–O$_t$ (terminal): 1.669(11)–1.701(10) Å; Mo–O$_b$ (bridge): 1.859(12)–1.948(12) Å; Mo–O$_c$ (central): 2.391(16)–2.475(18) Å. The bond valence sums (BVS) for the molybdenum atoms were calculated by using parameters given by Brown [14]. The results give the values of 5.81, 6.12, 5.92, 5.88, 5.92 and 6.09 for Mo(1)–Mo(6), which reveal that the oxidation state of the molybdenum atoms of the {PMo$_{12}$O$_{40}$} ion in **1** is +6. Therefore the formula of the {PMo$_{12}$O$_{40}$} is [PMo$_{12}^{VI}$O$_{40}$]$^{3-}$.

A feature of **1** is that the [PMo$_{12}$O$_{40}$]$^{3-}$ anion serves as a bi-dentate ligand coordinating to two nickel centers through the bonds between terminal oxygen atoms and the nickel atoms of the two [Ni(*Phen*)$_2$(H$_2$O)]$^{2+}$ TMCs which are disposed at the opposite sites of the [PMo$_{12}$O$_{40}$]$^{3-}$ anion, the Ni–O bond distance is 2.090(10) Å. Each Ni center not only receives the contribution of one terminal oxygen atom from the anion but also receives the contributions of four nitrogen atoms from two *Phen* ligands (Ni–N bonds: 2.043(11)–2.085(12) Å) as well as the contribution of one oxygen atom from a water molecule (Ni–Ow bond: 2.113(11)Å). Thus the nickel centers complete their octahedral coordination environments. In other words, the [PMo$_{12}$O$_{40}$]$^{3-}$ anion supports two [Ni(*Phen*)$_2$(H$_2$O)]$^{2+}$ TMCs with the Ni–O contacts, forming a novel POM bi-supported coordination unit {[PMo$_{12}$O$_{40}$][Ni(*Phen*)$_2$(H$_2$O)]$_2$}$^+$ with the Ni–Ni distance of 14.537(6) Å as shown in Fig. 1.

Table 2
The selected bond lengths of compounds **1** and **2**.

Compound **1**			
Mo(1)–O(5)	1.701(10)	Mo(4)–O(11)	1.910(12)
Mo(1)–O(16)	1.868(14)	MoMo(4)–O(17)	1.927(13)
Mo(1)–O(11)	1.905(14)	MoMo(4)–O(3)	2.455(17)
Mo(1)–O(9)	1.919(12)	Mo(5)–O(6)	1.696(11)
Mo(1)–O(13)	1.923(14)	Mo(5)–O(19)	1.880(14)
Mo(1)–O(2)	2.391(16)	Mo(5)–O(22)	1.886(13)
Mo(2)–O(7)	1.669(11)	Mo(5)–O(10)	1.902(13)
Mo(2)–O(17)	1.877(13)	Mo(5)–O(16)	1.910(13)
Mo(2)–O(10)	1.887(12)	Mo(5)–O(1)#1	2.455(14)
Mo(2)–O(18)	1.888(12)	Mo(6)–O(12)	1.669(12)
Mo(2)–O(14)	1.920(14)	Mo(6)–O(9)	1.859(12)
Mo(2)–O(3)	2.475(18)	Mo(6)–O(14)#1	1.864(14)
Mo(3)–O(21)	1.682(13)	Mo(6)–O(22)#1	1.926(13)
Mo(3)–O(18)#1	1.862(12)	Mo(6)–O(8)	1.948(12)
Mo(3)–O(13)	1.875(13)	Mo(6)–O(1)	2.433(18)
Mo(3)–O(20)#1	1.938(13)	Ni(1)–N(4)	2.043(11)
Mo(3)–O(19)	1.943(13)	Ni(1)–N(3)	2.056(13)
Mo(3)–O(3)#1	2.448(18)	Ni(1)–N(1)	2.065(12)
MoMo(4)–O(15)	1.699(12)	Ni(1)–N(2)	2.085(12)
MoMo(4)–O(8)	1.869(12)	Ni(1)–O(5)	2.090(10)
MoMo(4)–O(20)	1.879(13)	Ni(1)–OW1	2.113(11)

Symmetry code: #1: −x, −y+1, −z+1

Compound **2**			
W(1)–O(10)	1.648(17)	WMo(4)–O(11)	1.904(18)
W(1)–O(18)	1.865(16)	WMo(4)–O(19)#2	1.91(2)
W(1)–O(19)	1.880(17)	WMo(4)–O(3)#2	2.402(19)
W(1)–O(8)	1.913(17)	W(5)–O(7)	1.679(14)
W(1)–O(6)	1.927(15)	W(5)–O(13)	1.83(2)
W(1)–O(1)	2.42(2)	W(5)–O(11)	1.859(18)
W(2)–O(22)	1.660(16)	W(5)–O(15)	1.890(17)
W(2)–O(6)	1.844(15)	W(5)–O(9)	1.913(19)
W(2)–O(9)	1.894(18)	W(5)–O(2)	2.49(2)
W(2)–O(17)	1.895(16)	W(6)–O(20)	1.661(16)
W(2)–O(14)	1.934(17)	W(6)–O(8)	1.84(2)
W(2)–O(3)#2	2.39(2)	W(6)–O(21)	1.89(2)
W(3)–O(12)	1.654(17)	W(6)–O(16)	1.90(2)
W(3)–O(17)#2	1.866(18)	W(6)–O(15)	1.906(18)
W(3)–O(16)	1.90(2)	W(6)–O(2)	2.477(19)
W(3)–O(18)#2	1.925(16)	Cd(1)–N(2)	2.289(18)
W(3)–O(13)	1.941(18)	Cd(1)–N(3)	2.295(18)
W(3)–O(2)	2.42(2)	Cd(1)–N(4)	2.316(16)
WMo(4)–O(5)	1.684(15)	Cd(1)–N(1)	2.331(17)
WMo(4)–O(21)#2	1.852(17)	Cd(1)–Cl(1)	2.545(9)
WMo(4)–O(14)	1.86(2)	Cd(1)–Cl(1)#3	2.724(9)

Symmetry code: #2: −x+1/2, −y+3/2, −z+1; #3: −x,y, −z+3/2
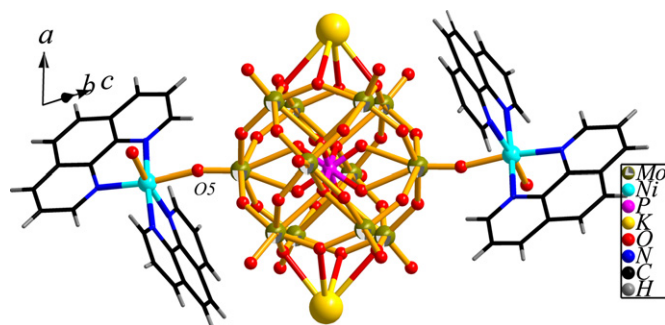
Fig. 1. The ball-and-stick and wire representation of the POM bi-supported coordination unit {[PMo$_{12}$O$_{40}$][Ni(*Phen*)$_2$(H$_2$O)]$_2$}$^+$.

Another feature of **1** is that the POM [PMo$_{12}$O$_{40}$]$^{3-}$ not only serves as a bidentate ligand coordinating to two nickel centers, more importantly, but also acts as building block connected by K$^+$ cations into a novel 1-D straight chain structure. The K$^+$ cations of **1**, exhibiting a bitetragonal bipyramidal coordination environment, receives contributions not only from four oxygen donors from a POM [PMo$_{12}$O$_{40}$]$^{3-}$ but also from four oxygen donors from

an adjacent [PMo$_{12}$O$_{40}$]$^{3-}$ POM (Ni–O bond distance: 2.75(1)– 2.95(2) Å). Thus the K$^+$ cations in **1** act as bridges interconnecting the neighboring [PMo$_{12}$O$_{40}$]$^{3-}$ POMs through the K–O contacts into a novel straight chain structure along the *b*-axis (Fig. 2).

Detailed analysis revealed that there contains a (H$_6$O$_4$)$^{2-}$ unit in **1**, which is constructed from two hydroxyl ions O23 and two coordination water molecules Ow1, as shown in Fig. 3. The O23 interacts with the O23a with hydrogen bonding interaction of 3.04(2) Å into a "rod" shaped dinuclear unit with the O23 at one side and the O23a at the other side of the "rod". The O23 interacts with the Ow1 at one side with hydrogen bonding interaction of 2.72(2) Å, while the O23a interacts with the Ow1a at the other side with the hydrogen bonding interaction of 2.72(2) Å, too. Thus a zig-zag chain (H$_6$O$_4$)$^{2-}$ unit is formed.

For the Ow1 coordinates to the nickel centers, the (H$_6$O$_4$)$^{2-}$ acts as bridges interconnecting the neighboring straight chains into a 2-D supramolecular layer structure. Detailed analysis also revealed that there exist hydrogen bonding interactions between the oxygen atoms of the (H$_6$O$_4$)$^{2-}$ units and the oxygen atoms of the [PMo$_{12}$O$_{40}$]$^{3-}$ ions with O23...O11 distance of 2.94(2) Å.

It should be noted that an isostructural compound was reported by our group before [15]. The biggest difference between compound **1** and the reported one is the building block: the former is [PMo$_{12}$O$_{40}$]$^{3-}$, and the latter is [PW$_{12}$O$_{40}$]$^{3-}$.

3.1.2. Crystal structure of compound 2

Single-crystal X-ray diffraction analysis reveals that compound **2** is constructed from Pseudo-Keggin polyoxoanions [HPW$_{12}$O$_{40}$]$^{2-}$, cadmium complex cations [Cd$_2$(*Phen*)$_4$Cl$_2$]$^{2+}$ and water molecules of crystallization. The [HPW$_{12}$O$_{40}$]$^{2-}$ is an isostructural tungsten analog of the [PMo$_{12}$O$_{40}$]$^{3-}$ ion in **1**. According to the different coordination environments, oxygen atoms can be divided into three groups: W–O$_t$, W–O$_b$ and W–O$_c$ bonds with bond distances falling in the ranges of 1.648(17)–1.684(15), 1.83(2)–1.941(18) and 2.39(2)–2.42(2) Å, respectively. The P–O distances are in the range of 1.48(2)–1.61(2) Å. The bond valence sums (BVS) for tungsten atoms were calculated by using parameters given by Brown [14]. The results give the values of 6.00, 6.01, 5.96, 6.01, 6.01 and 6.00 for W(1)–W(6), which reveal that the oxidation state of the tungsten atoms of the {PW$_{12}$O$_{40}$} in **2** is +6. So the formula of the {PW$_{12}$O$_{40}$} is [HPW$_{12}$O$_{40}$]$^{2-}$. It should be noted that the hydrogen atom attached to the POM could not be located by the crystallographic analysis.

An unusual feature of **2** is that it contains a novel [Cd$_2$(*Phen*)$_4$Cl$_2$]$^{2+}$ TMC. It is not a simple metal–ligand coordination complex, but contains two chloride ions coordinating to the cadmium centers. Each Cd ion is coordinated by four nitrogen atoms from two *Phen* ligands with bond distances of 2.289(18)–2.331(17) Å, forming a [Cd(*Phen*)$_2$]$^{2+}$ TMC. Two [Cd(*Phen*)$_2$]$^{2+}$ TMCs are linked by two chloride ions with bond distance of 2.545(9)–2.724(9) Å, forming a novel dimer formulated as [Cd$_2$(*Phen*)$_2$Cl$_2$]$^{2+}$. Alternatively The chloride ions serves as inorganic bridges joining the two [Cd(*Phen*)$_2$]$^{2+}$ TMCs into a novel metal–chloride–ligand coordination complex or a novel metal chloride cluster. As shown in Fig. 4, the novel cluster [Cd$_2$(*Phen*)$_4$Cl$_2$]$^{2+}$ exhibits a very beautiful "butterfly" motif. This feature is reminiscent of a similar "butterfly" cluster {[Cd(*Phen*)$_2$]$_2$ Cl}$^{3+}$ prepared by our group very recently [16]. However, a detailed study of the two "butterfly" clusters reveals that there exists significant difference between them. The cluster {[Cd(*Phen*)$_2$]$_2$Cl}$^{3+}$ contains only one chloride ion bridging two [Cd(*Phen*)$_2$]$^{2+}$ cations. In contrast to the cluster {[Cd(*Phen*)$_2$]$_2$Cl}$^{3+}$, it is very strange to observe that the cluster [Cd$_2$(*Phen*)$_4$Cl$_2$]$^{2+}$ in compound **2** contains two chloride ions as double bridges. The reason why they contain different chloride ions is still elusive. To the best of our knowledge, such metal chloride cluster [Cd$_2$(*Phen*)$_4$Cl$_2$]$^{2+}$ has never been reported before.
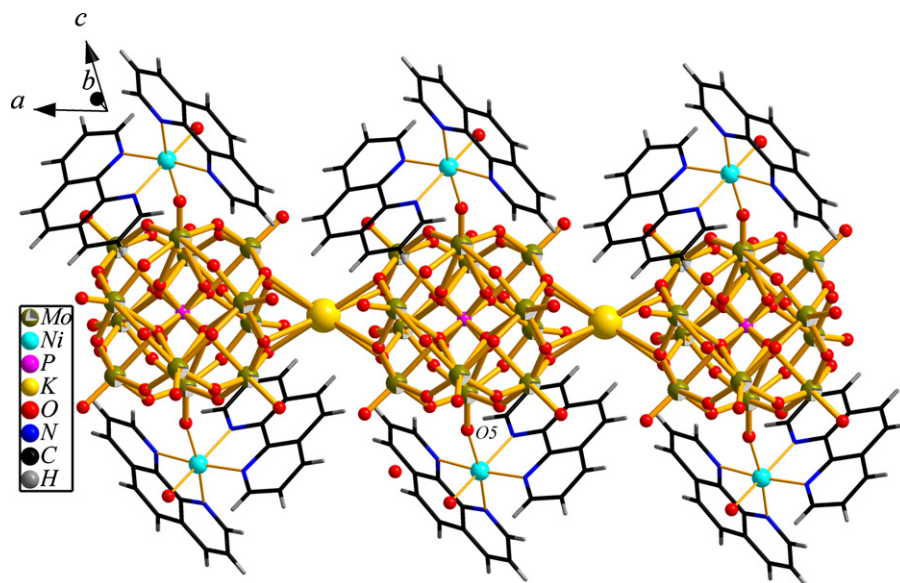
Fig. 2. The 1-D chain structure constructed from Keggin POM supported transition metal coordination fragments linked by potassium ions.
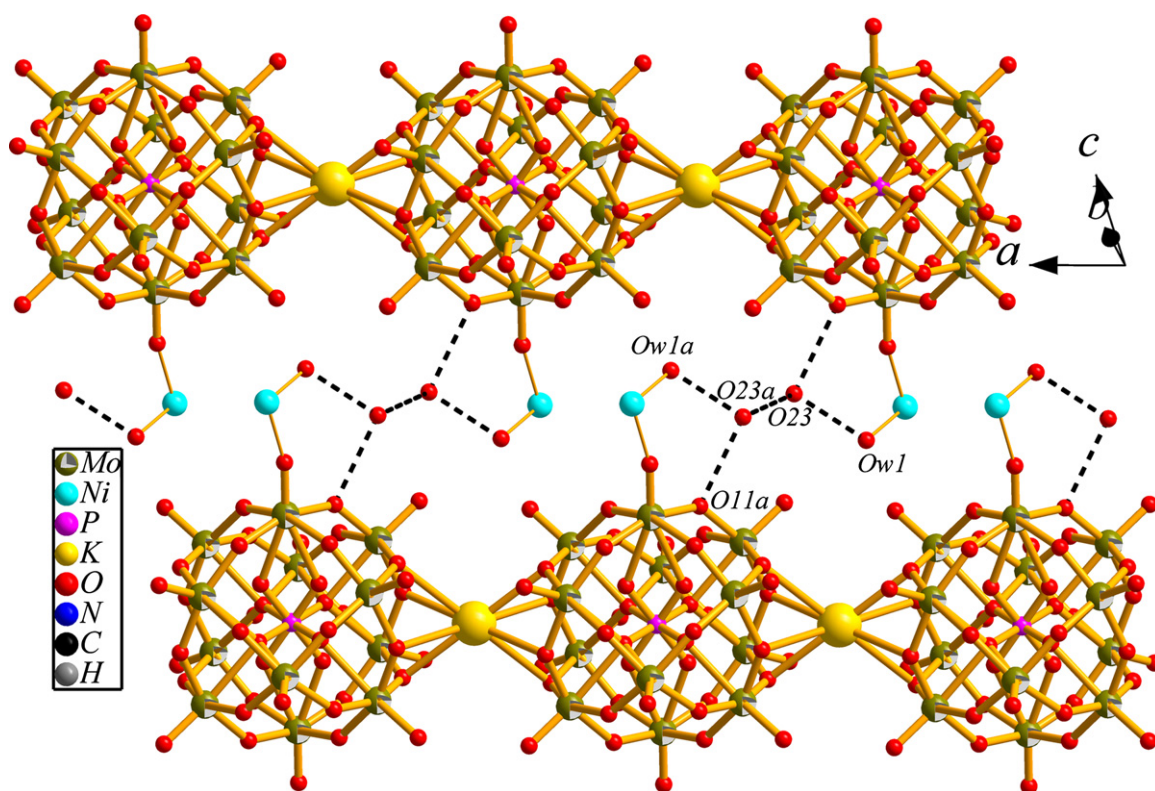

Fig. 3. The hydrogen bonds between the hydroxyl ions and the water molecules and the terminal oxygen atoms of the $[PMo_{12}O_{40}]^{3-}$. Symmetry code—a: $(1-x, 1-y, -z)$.

The role of the two "butterfly" clusters in the packing structure is thoroughly different. The cluster $\{[Cd(Phen)_2]_2Cl\}^{3+}$ acting as bridges interconnect the $[PMo_{12}Sb_2O_{40}]^{3-}$ POMs into a novel chain structure. However, the "butterfly" cluster $[(Cd(Phen)_2)_2Cl_2]^{2+}$ in **2** interacts with the terminal oxygen atoms of the $[HPW_{12}O_{40}]^{2-}$ POMs with Cd–O contact of 3.64(2) Å, which means very weak interactions.

Detailed analysis revealed that there exist complex hydrogen bonds between the oxygen atoms of the $[HPW_{12}O_{40}]^{2-}$ POMs and

the carbon atoms of the "butterfly" clusters $[(Cd(Phen)_2)_2Cl_2]^{2+}$. The C(17) interacts with the O(12)(0.5–x,1.5–y,1–z) through hydrogen bond with bond distance of 3.15(4) Å, the C(10) interacts with the O(22) through hydrogen bond with bond distance of 3.19(3) Å, while the C(15) interacts with the O(5)(0.5 – x, –0.5+y,1.5 – z) through hydrogen bond with bond distance of 2.95(3) Å. These complex hydrogen bonds and their symmetry equivalents connect the $[HPW_{12}O_{40}]^{2-}$ POMs and the "butterfly" clusters $[(Cd(Phen)_2)_2Cl_2]^{2+}$ into a 3-D supramolecular structure, as shown in Fig. S1.
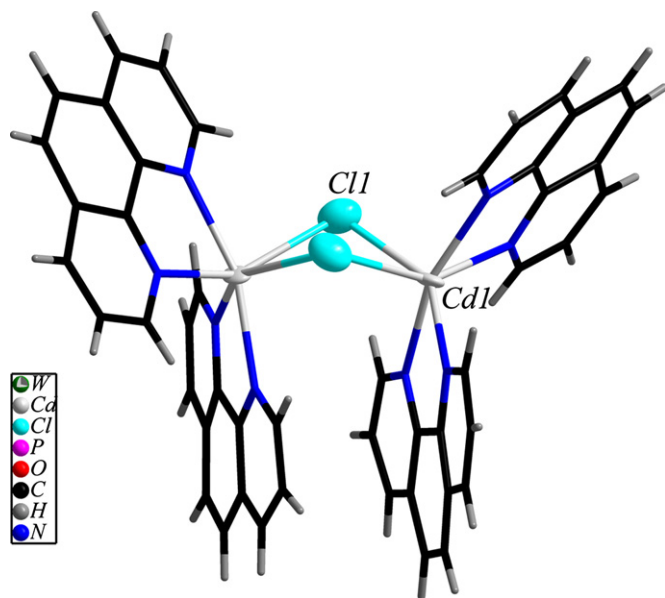
Fig. 4. The wire representation the of the $[Cd_2(Phen)_4Cl_2]^{2+}$.

3.2. Characterization of the compounds

In the IR spectrum for compound **1**, the peak at 1056 cm^{-1} is associated with the asymmetric vibrations of the P–O units. The peaks at 957 and 870 cm^{-1} are due to υ(Mo–O$_t$) and υ(Mo–O$_b$–Mo), respectively, and those at 812 and 723 cm^{-1} are due to υ(Mo–O$_c$). A series of bands in the range 100–1625 cm^{-1} are characteristic of the Phen ligands in compound **1**. The IR spectrum for compound **2** is similar to that of **1**. The peaks at 974 cm^{-1} is associated with the υ(W–O$_t$), 892 cm^{-1} is attributed to υ(W–O$_b$–W), and those at 815 and 723 cm^{-1} are related to υ(W–O$_c$). Bands at 1078 cm^{-1} can be ascribed to P–O stretching vibrations in **2**. Bands in the 1100–1624 cm^{-1} region are due to vibrations of the Phen ligands in **2**.

Fig. S2(a) shows the XPS spectrum for **1** as two peaks at 232.3 and 235.2 eV ascribed to Mo^{6+} 3d5/2 and Mo^{6+} 3d3/2. The XPS spectrum for **2** gives two peaks at 35.6 and 37.8 eV attributed to W^{6+} 4f7/2 and W^{6+} 4f5/2, respectively (Fig. S2(b)). The XPS estimation of the valence is in reasonable agreement with those calculated from bond valence sum calculations of compounds **1** and **2**.

The powder X-ray diffraction pattern for **1** and **2** are both in good agreement with the ones simulated based on the data of the single-crystal structures, indicating the purity of the as-synthesized products (Fig. S3). The differences in reflection intensity are probably due to preferred orientations in the powder samples of compounds **1** and **2**.

The UV–vis spectra of compounds **1–2**, in the range 260–450 nm, are presented in Fig. S4. The UV–vis spectrum of compound **1** displays wide medium intense absorption peaks at about 273 and 330 nm assigned to O→Mo charge transfer in the polyoxoanion structure. The UV–vis spectrum of compound **2** exhibits wide medium intense absorption peak at 266 and 328 nm attributed to charge transfer bands of O→W in the polyoxoanion structure.

4. Conclusion

Two new compounds based on Keggin-type POMs have already been synthesized and characterized. Compound **1** is a 1-D chain structure which is constructed from Keggin POM supported transition metal coordination fragments linked by alkali metals. Compound **2** is constructed from Keggin POMs

and transition metal–halide–organic coordination units. It is well-known that POMs combined with TMCs is a popular field of POMs, however, POMs combined with both TMCs and other elements like alkali metals or halide ions is seldom reported, and compounds **1** and **2** give two good examples of such compounds.

Appendix A. Supporting information

Supplementary data associated with this article can be found in the online version at doi:10.1016/j.jssc.2011.01.009.

References

[1] M.T. Pope, Heteropoly and Isopoly Oxometalates, Springer-Verlag, Berlin, 1983.
[2] (a) M.T. Pope, A. Müller, Angew. Chem. Int. Ed. Engl. 30 (1991) 34;
    (b) Chem. Rev. 98 (1998) 1.
[3] M.T. Pope, A. Müller, Polyoxometalates: From Platonic Solids to Anti-Retro Viral Activity, Kluwer, Dordrecht, The Netherlands, 1994.
[4] M.T. Pope, A. Müller (Eds.), Polyoxometalate Chemistry: From Topology via Self-Assembly to Applications, Kluwer, Dordrecht, The Netherlands, , 2001.
[5] T. Yamase, M.T. Pope (Eds.), Polyoxometalate Chemistry for Nano-Composite Design, Kluwer, Dordrecht, The Netherlands, 2002.
[6] P.J. Hagrman, D. Hagrman, J. Zubieta, Angew. Chem. Int. Ed. Engl. 38 (1999) 2638.
[7] (a) J.Q. Xu, R.Z. Wang, G.Y. Yang, Y.H. Xing, D.M. Li, W.M. Bu, L. Ye, Y.G. Fan, G.D. Yang, Y. Xing, Y.H. Lin, H.Q. Jia, Chem. Commun. (1999) 983;
    (b) Y. Xu, J.Q. Xu, K.L. Zhang, Y. Zhang, X.Z. You, Chem. Commun. (2000) 153;
    (c) J.X. Chen, T.Y. Lan, Y.B. Huang, C.X. Wei, Z.S. Li, Z.C. Zhang, J. Solid State Chem. 179 (2006) 1904;
    (d) J.W. Cui, X.B. Cui, H.H. Yu, J.Q. Xu, Z.H. Yi, W.J. Duan, Inorg. Chim. Acta 361 (2008) 2641;
    (e) D. Xiao, Y. Hou, E. Wang, S. Wang, Y. Li, L. Xu, C. Hu, Inorg. Chim. Acta 357 (2004) 2525;
    (f) C.M. Liu, D.Q. Zhang, D.B. Zhu, Cryst. Growth Des. 3 (2003) 363.
[8] (a) M.I. Khan, E. Yohannes, R.J. Doedens, Angew. Chem. Int. Ed. 38 (1999) 1292;
    (b) J. Lu, Y. Xu, N.K. Goh, L.S. Chia, Chem. Commun. (1998) 2733;
    (c) A. Tripathi, T. Hughbanks, A. Clearfield, J. Am. Chem. Soc. 125 (2003) 10528;
    (d) J.R.D. Debord, R.C. Haushalter, L.M. Meyer, D.J. Rose, P.J. Zapf, J. Zubieta, Inorg. Chim. Acta 256 (1997) 165;
    (e) P.J. Hagrman, D. Hagrman, J. Zubieta, Angew. Chem. Int. Ed. 38 (1999) 2638;
    (f) D. Hagrman, C. Zubieta, D.J. Rose, J. Zubieta, R.C. Haushalter, Angew. Chem. Int. Ed. 36 (1997) 873;
    (g) A. Dolbecq, P. Mialane, L. Lisnard, J. Marrot, F. Sécheresse, Chem. Eur. J. 9 (2003) 2914;
    (h) P. Mialane, A. Dolbecq, F. Sécheresse, Chem. Commun. (2006) 3477;
    (i) S. Reinoso, P. Vitoria, J.M. Gutiérrez-Zorrilla, L. Lezama, L. San Felices, J.I. Beitia, Inorg. Chem. 44 (2005) 9731;
    (j) J. Thomas, A. Ramanan, Cryst. Growth Des 8 (2008) 3391;
    (k) K. Pavani, S.E. Lofland, K.V. Ramanujachary, A. Ramanan, Eur. J. Inorg. Chem. (2007) 568.
[9] (a) C. Lei, J.G. Mao, J.Q. Sun, J.L. Song, Inorg. Chem. 43 (2004) 1964;
    (b) C. Liu, D. Zhang, M. Xiong, D. Zhu, Chem. Commun. (2002) 1416;
    (c) Y.P. Ren, X.J. Kong, X.Y. Hu, M. Sun, L.S. Long, R.B. Huang, L.S. Zheng, Inorg. Chem. 45 (2006) 4016;
    (d) G.C. Qu, L. Jiang, X.L. Feng, T.B. Lu, Dalton Trans. (2009) 71;
    (e) J.Y. Niu, D.J. Guo, J.P Wang, J.W. Zhao, Cryst. Growth Des. 4 (2004) 241;
    (f) C.M. Liu, J.L. Luo, D.Q. Zhang, N.L. Wang, Z.J. Chen, D.B. Zhu, Eur. J. Inorg. Chem. (2004) 4774;
    (g) C.M. Liu, D.Q. Zhang, M. Xiong, D.B. Zhu, Chem. Commun. (2002) 1416.
[10] (a) X.B. Cui, J.Q. Xu, H. Meng, S.T. Zheng, G.Y. Yang, Inorg. Chem. 43 (2004) 8005;
    (b) X.B. Cui, Y.Q. Sun, G.Y Yang, Inorg. Chem. Commun. 6 (2003) 259;
    (c) C. Pan, J. Xu, G. Li, X. Cui, L. Ye, G. Yang, Dalton Trans. (2003) 517;
    (d) X.B. Cui, J.Q. Xu, Y. Li, Y.H. Sun, G.Y. Yang, Eur. J. Inorg. Chem. 43 (2004) 1051;
    (e) S.T. Zheng, J. Zhang, G.Y. Yang, Angew. Chem. Int. Ed. 47 (2008) 3909;
    (f) J.W. Zhao, C.M. Wang, J. Zhang, S.T. Zheng, G.Y. Yang, Chem. Eur. J. 14 (2008) 9223.
[11] (a) H.Y. An, Y.G. Li, E.B. Wang, D.R. Xiao, C.Y. Sun, L. Xu, Inorg. Chem. 44 (2005) 6062;
    (b) H.Y. An, E.B. Wang, D.R. Xiao, Y.G. Li, Z.M. Su, L. Xu, Angew. Chem. Int. Ed. 45 (2006) 904;
    (c) J. Lü, E.H. Shen, Y.G. Li, D.R. Xiao, E.B. Wang, L. Xu, Cryst. Growth Des. 5 (2005) 65;
    (d) C.Y. Sun, Y.G. Li, E.B. Wang, D.R. Xiao, H.Y. An, L. Xu, Inorg. Chem. 46 (2007) 1543;

  (e) Y. Lu, Y. Xu, E.B. Wang, X.X. Xu, Y. Ma, Inorg. Chem. 45 (2006) 2060;
  (f) H.Y. An, Y.G. Li, D.R. Xiao, E.B. Wang, C.Y. Sun, Cryst. Growth Des. 6 (2006) 1107.
[12] (a) P.Q. Zheng, Y.P. Ren, L.S. Long, R.B. Huang, L.S. Zheng, Inorg. Chem. 44 (2005) 1190;
  (b) X.L. Wang, C. Qin, E.B. Wang, Y.G. Li, N. Hao, C.W. Hu, L. Xu, Inorg. Chem. 43 (2004) 1850;
  (c) C.P. Pradeep, D.L. Long, G.N. Newton, Y.F. Song, L. Cronin, Angew. Chem. Int. Ed. 47 (2008) 4388;
  (d) Z.H. Yi, X.B. Cui, X. Zhang, G.D. Yang, J.Q. Xu, X.Y. Yu, H.-H. Yu, W.J. Duan, J. Mol. Struct. 891 (2008) 123;
  (e) T.R. Veltman, A.K. Stover, A.N. Sarjeant, K.M. Ok, P.S. Halasyamani, A.J. Norquist, Inorg. Chem. 45 (2006) 5529;
  (f) R. Atencio, A. Briéno, X. Galindo, Chem. Commun. (2005) 637;
  (g) R. Atencio, A. Bricéno, P. Silva, J.A. Rodríguez, J.C. Hanson, New J. Chem. 31 33 (2007);
  (h) R. Dessapt, M. Collet, V. Coué, M. Bujoli-Doeuff, S. Jobic, C. Lee, M.H. Whangbo, Inorg. Chem. 48 (2009) 574;
  (i) R.Q. Fang, Y.F. Zhao, X.M. Zhang, Inorg. Chim. Acta 359 (2006) 2023.

[13] (a) Y. Wang, L. Ye, T.G. Wang, X.B. Cui, S.Y. Shi, G.W. Wang, J.Q. Xu, Dalton Trans. 39 (2010) 1916;
  (b) X.F. Kuang, X.Y. Wu, R.M. Yu, J.P. Donahue, J.S. Huang, C.Z. Lu, Nat. Chem. 2 (2010) 461;
  (c) L. Yuan, C. Qin, X.L. Wang, Y.G. Li, E.B. Wang, Dalton Trans. (2009) 4169;
  (d) X. Zhang, Z.H. Yi, L.Y. Zhang, Q. Chen, X.M. Gu, J.Q. Xu, X.L. Wang, C. Yang, X.Z. Xu, W.J. Xia, Dalton Trans. (2009) 9198;
  (e) F. Yu, X.J. Kong, Y.Y. Zheng, Y.P. Ren, L.S. Long, R.B. Huang, L.S. Zheng, Dalton Trans. (2009) 9503.
[14] I.D. Brown, in: M. O'Keefe, A. Navrotsky (Eds.), Structure and Bonding in Crystals, vol. 2, Academic Press, New York, 1981, pp. 1–30.
[15] J.W. Cui, X.B. Cui, H.H. Yu, J.Q. Xu, Z.H. Yi, W.J. Duan, Inorg. Chim. Acta 361 (2008) 2641.
[16] L.N. Xiao, Y. Peng, Y. Wang, Z.M. Gao, Y.B. Liu, D.F. Zheng, X.B. Cui, J.Q. Xu. Euro. J. Inorg. Chem. accepted for publication.